www.czasopisma.pan.pl PAN POLSKA AKADEMIA NAUK www.journals.pan.pl

Arch. Metall. Mater. **68** (2023), 2, 775-783

DOI: https://doi.org/10.24425/amm.2023.142461

ASHISH KUMAR[1*], RAVINDRA SINGH RANA[1],
RAJESH PUROHIT[1], ANURAG NAMDEV[1]

OPTIMIZATION OF T-6 CYCLE AND CHARACTERIZATION OF Si_3N_4 REINFORCED HIGH STRENGTH ALUMINUM METAL MATRIX COMPOSITES

In this research, AA7068/Si_3N_4 composites were fabricated through stir casting with the attachment of ultrasonic treatment. The quenching medium and aging duration significantly influenced the hardness of Al alloy samples. Peak hardness was achieved after 12 h of artificial aging at the temperature of 140°C. The addition of nano Si_3N_4 significantly refined the microstructure of unreinforced AA7068. The dispersion of intermetallic compounds ($MgZn_2$) and grain boundary discontinuation were noticed after the T-6 heat treatment. Ultimate tensile strength, yield strength, and hardness were improved by 70.95%, 76.19%, and 44.33%, respectively, with the addition of 1.5 weight % Si_3N_4 compared to as-cast alloy due to the combined effect of heat treatment, hall-Petch, Orowan, thermal miss match, load-bearing strengthening mechanisms and uniform dispersion of reinforcement. A reduction in percentage elongation was noticed due to composites' brittle nature by the effect of ceramic Si_3N_4 particles' inclusion. The fracture surfaces reveal ductile failure for alloy and mixed-mode failure in the case of composites.

Keywords: Stir casting; Microstructure; Mechanical properties; Optimization; fractography

1. Introduction

In the new era of advanced materials, aluminum alloys attract researchers due to their high strength-to-weight ratio, lower thermal expansion, excellent mechanical properties, and resistance to corrosion and wear. Despite these properties, higher mechanical and wear resistance is required for automotive, aerospace, and industrial applications [1] and [2]. To increase mechanical and wear properties, ceramic particles like SiC [3], B4C [4], TiC [5], Al2O3 [6], Gr [7], GNP [8], MWCNT [9], Si_3N_4 [10] were used as reinforcement in aluminum alloys.

7xxx Al-Zn-Mg-Cu alloys have commonly been used as high-strength and heat treatable alloys for automotive, aerospace, transportation, and marine applications due to their excellent machinability, formability, and corrosion protection and wear resistance. AA7068 alloy is utilized in automobile and aerospace, having excellent strength with anti corrosive properties and high resistance to wear and workability. It is widely utilized in developing connecting rods, piston rings, valves, cylinder liners, cranes, and roofs [11,12]. T-6 Heat treatment is a promising route to enhance the mechanical and wear properties of 7xxx Al-Zn-Mg-Cu alloys [13,14].

J.M. Mistry et al. [15] developed Al7075/Si_3N_4 composites through a stir casting approach with varying Si_3N_4 weight % such as 4, 8, and 12 wt. %. They noticed superior hardness and tensile strength in heat-treated composites and alloys, as well as these properties were also increased after adding Si_3N_4 particles in Al7075 alloy. Tensile strength was optimized at 8 wt. % and started decreasing due to the increased porosity and clustering of reinforcing particles. P. Sharma et al. [16] analyzed the mechanical properties of Si_3N_4 reinforced Al 6082-T6 composites. They developed composites with 2, 4, 6, 8, 10, and 12 wt. % Si_3N_4 and observed enhancement in tensile strength with the addition of Si_3N_4 particles from 2 to 10 wt. %. Rajkumar et al. [17] analyzed the changes in hardness behavior after the addition of SiC particles in Al-Si alloy using stir casting route, they found a significant increment in hardness value with reinforcement attributed to the hard nature of SiC. Mechanical properties were affected at 12 wt. % due to the ununiform distribution of reinforcement. Other studies on Si_3N_4 reinforced Al alloy composites revealed that hardness, tensile, compressive, and impact strength were increasing with an increase in wt. % of Si_3N_4 [18,19] and [20]. In contrast, mechanical properties were compromised at a higher weight % due to uneven distribution,

[1] MAULANA AZAD NATIONAL INSTITUTE OF TECHNOLOGY, DEPARTMENT OF MECHANICAL ENGINEERING, BHOPAL, MADHYA PRADESH, INDIA

* Corresponding author: bhaskar.171ashish@gmail.com

clustering, and casting defects. Incorporating ceramic SiC particles in al alloy improves the mechanical and tribological properties, and wear resistance is significantly enhanced with the addition of reinforcement [21,22].

The present work included the fabrication of Si_3N_4 reinforced AA7068 nanocomposites using stir casting with ultrasonic treatment. T-6 heat-treatment cycle parameters such as quenching medium and aging time were optimized for AA7068, and the optimized parameters were used further. Si_3N_4 particles in the proportion of 0.5 to 2 wt. % in step of 0.5 incorporated in AA7068 to develop nanocomposites. The microstructure of Si_3N_4 developed composites and fractured surfaces were analyzed through EDS, FESEM, and elemental mapping.

2. Research methodology

2.1. Selection of materials

High-strength Al 7078 alloy has been selected as a metal matrix; the identified set of alloying elements is presented in TABLE 1. Zn is present in Al alloy as a major alloying element (7.8 wt. %), followed by Mg (3.1 wt. %) and Cu (1.2 wt.%). Silicon nitride (Si_3N_4) was selected as reinforcing ceramic in particulate form (average size is 58.32 nm), purchased from nano research elements. Silicon nitride is a ceramic material with unique properties, such as being very hard in nature, high melting point, low density (3.19 g/cc), and resistance at higher temperatures. The SEM and EDS of Si_3N_4 are shown in Fig. 1. The weight % of Si and N elements in Si_3N_4 are 54.23 and 45.77.

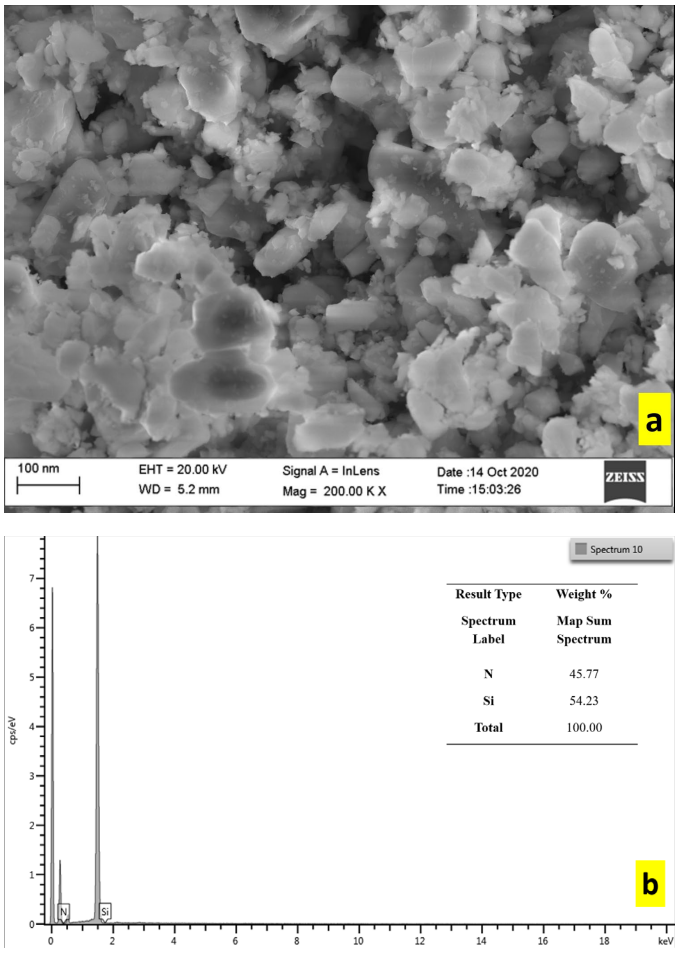

Fig. 1 (a) FESEM image of Si_3N_4, (b) EDS of Si_3N_4

2.2. Fabrication process

Firstly, mechanical alloying was performed on Al and Si_3N_4 powder using a planetary ball miller (Amaze instruments VPB-2 Model) at a lower speed of 250 rpm for 4 h to increase the wettability between reinforcement and molten alloy. In mechanical milling operation, one part Al and three part Si_3N_4 powder were taken into consideration to maintain the ratio of 1:3 by volume. Stainless steel balls (10 mm diameter) were used, and jars were filled only 1/3rd of their volume to ensure proper powder mixing. Isopropyl alcohol was used as a cooling agent to prevent the mixture from excessive heating. It has been observed that the molten Al alloy rejected nanoparticles at the time of mixing due to the higher surface area, surface energy, and less wettability, so ball milled (Al and Si_3N_4) powder was used for better mixing and distribution. Prepared ball milled powder was preheated at 350°C to remove moisture and ready to be used as a filler in molten AA7068.

Secondly, the fabrication of Si_3N_4 strengthened AA7068 nanocomposites was done through a stir casting method equipped with an ultrasonic treatment facility. Electrical resistance furnaces were used to melt the ingots of AA7068 at 780°C with a heating rate of 10°C per second. After melting, coverall-11 was mixed by 1 wt. % to make melt slag free, followed by mixing Mg pieces (2 wt. %) to improve the wettability. Preheated ball milled powder was mixed in the molten alloy in three steps with the continuation of stirring at 500 rpm. Agglomeration of nano reinforcement was prevented by ultrasonic treatment, in which a niobium probe was used to transfer the ultrasonic waves at 20 Hz for minutes for uniform distribution and better mechanical properties [23]. Later the prepared mixture was poured into the preheated mold. The nanocomposites were prepared by varying the Si_3N_4 weight % from 0.5 to 2. Samples for microstructure analysis and tensile and hardness testing were prepared for all compositions. Later the optimized T-6 heat treatment was performed on the samples. The prepared samples of all compositions with their designation are shown in TABLE 1.

TABLE 1

Compositions of material with the designation

Sample	Type of material	Designation
1.	As-cast AA7068	ACA
2.	Heat-treated AA7068	HTA
3.	Heat treated AA7068 + 0.5 wt.% Si_3N_4	HT-1
4.	Heat treated AA7068 + 1.0 wt.% Si_3N_4	HT-2
5.	Heat treated AA7068 + 1.5 wt.% Si_3N_4	HT-3
6.	Heat treated AA7068 + 2.0 wt.% Si_3N_4	HT-4

2.3. Heat treatment

AA7068 was subjected to a T-6 heat treatment cycle to enhance the mechanical properties. For superior mechanical properties of composites, peak aging condition was identified by optimizing the T-6 heat treatment parameters such as quenching medium and aging time. Fig. 2 shows the T-6 cycle, which comprises solution treatment followed by artificial aging. Firstly two batches of 12 samples of Al alloy were heated up to 490°C for 6h, followed by sudden quenching in water and oil medium separately. Later these solutionized samples were artificially aged at 140°C [24] for 2, 4, 6, 8, 10, 12, 14, 16, 18, 20, 22, and 24 h, followed by natural cooling in air. Hardness is measured for water and oil quenched samples.

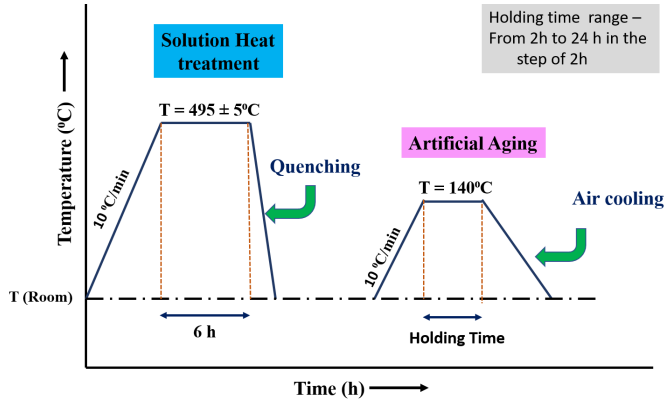

Fig. 2. Schematic diagram of the T-6 cycle

For each condition, hardness was measured by considering the average of five values, and the optimized heat treatment parameter was identified. All compositions (shown in TABLE 1) were heat-treated at the optimized condition, and mechanical properties were evaluated.

3. Result and discussion

3.1. Microstructure analysis

The morphology of Al-Si_3N_4 mixture after ball milling is shown in Fig. 3(a). It is noticed that Si_3N_4 particles were broken due to shear forces applied by steel balls during the milling

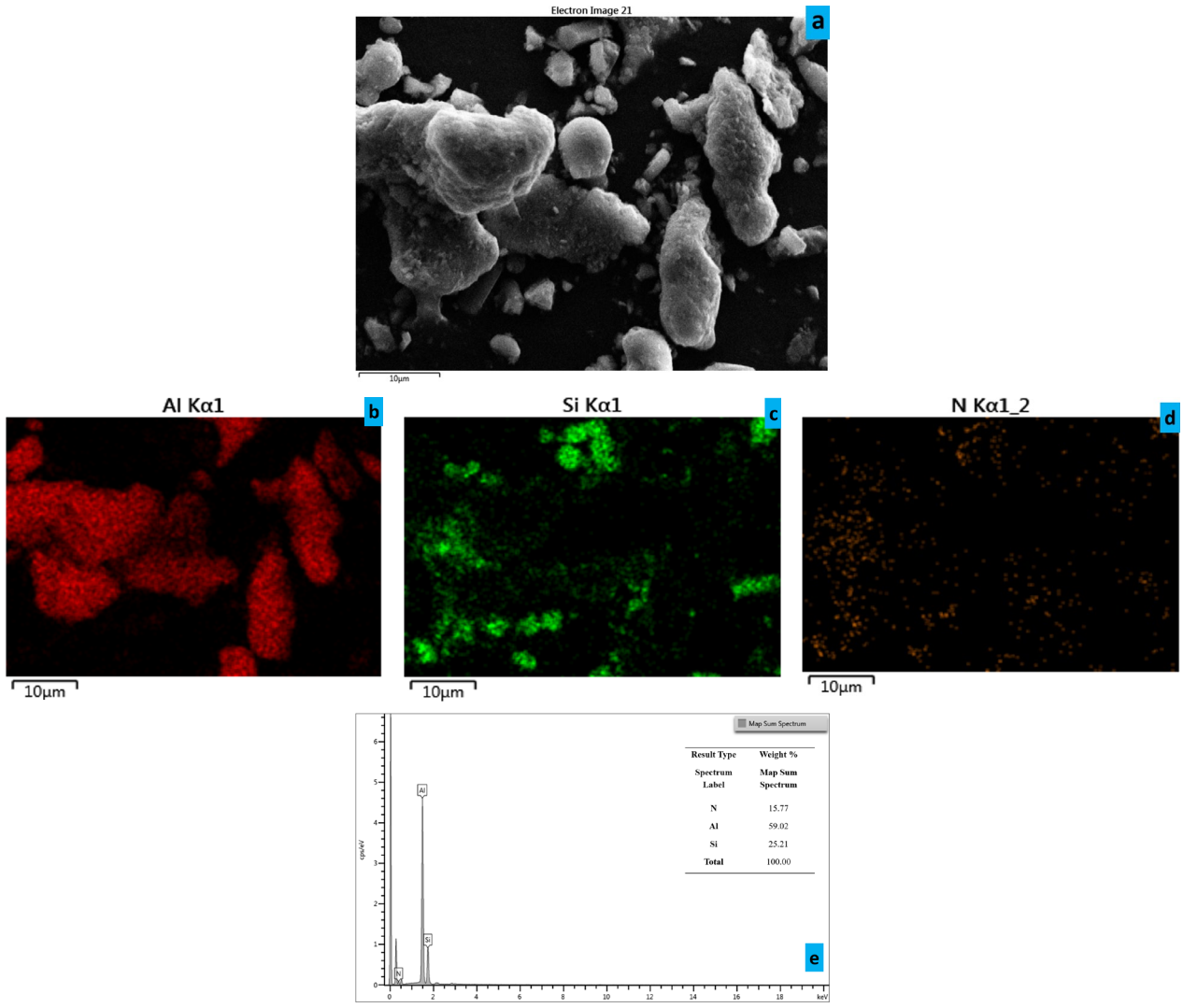

Fig. 3. (a) SEM of ball-milled powder (b,c, and d) identification of Al, Si, and N respectively through Elemental Mapping (e) EDS of ball-milled powder

process; repeated fracturing and welding were associated with the Al-Si_3N_4 mixture. Steric acid (2 wt. %) was added to the mixture to avoid cold welding and destruction of Si_3N_4 particles to achieve uniform dispersion of reinforcing particles on the Al surface. The elemental mapping of ball-milled powder (shown in Fig. 3(a to d) identified the elements such as Al, Si, and N through unique colors. EDS also identified the present elements through their respective peaks shown in Fig. 2(e). The microstructure of AA7068 with and without heat treatment is shown in Fig. 4((a) and (b)). Whereas the microstructure of heat-treated and Si_3N_4 reinforced nanocomposites are shown in Fig. 4((c) and (d)). A continuous eutectic phase separates coarser α-Al grains, and intermetallic compounds such as Al $(Zn, Cu, Mg)_2$ were observed after the solidification of ACA. In comparison, the discontinuous grain boundaries and MgZ_2 precipitates were observed in the microstructure of HTA. In addition, significant refinement of coarser grain was noticed after Si_3N_4 nano reinforcement with uniform distribution of fine MgZ_2 particles in the case of HT-3. Clustering of particles and microvoids was observed in the microstructure of HT-4 due to the higher surface area and low density of Si_3N_4 nanoparticles. The higher surface area and surface energy of nanoparticles increase the agglomeration behavior of particles. Grains of ACA were significantly refined with the addition of nano reinforcement up to 2 wt. %. The grain refinement could be related to the fact that Si_3N_4 particles act as a secondary phase in primary Al matrix sites and the formation of nuclei starts from these sites; the growth of the grain is hindered by the nearest Si_3N_4 particles [25].

Fig. 5 represents the Energy dispersive x-ray spectroscopy (EDS) of ACA, HT-3, and HT-4. Alloying elements such as Zn, Mg, Cu, Fe, and Si are identified with their respective peak shown in Fig. 5(a). In comparison, elements presented in Si_3N_4, such as Si and N, are additionally confirmed with alloying elements by EDS (shown in Fig. 5(b) and (c). The increasing amount of reinforcement and weight % of each element displaying in the table attached to the EDS plot. EDS has been carried out on CARL ZEISS EVO (IIT, Kanpur) instrument with 15 kV accelerating voltage and 5×10^4 magnification.

3.2. Density and porosity

Comparative density and porosity % of as-cast and heat-treated alloy and nanocomposites are represented in Fig. 6. The

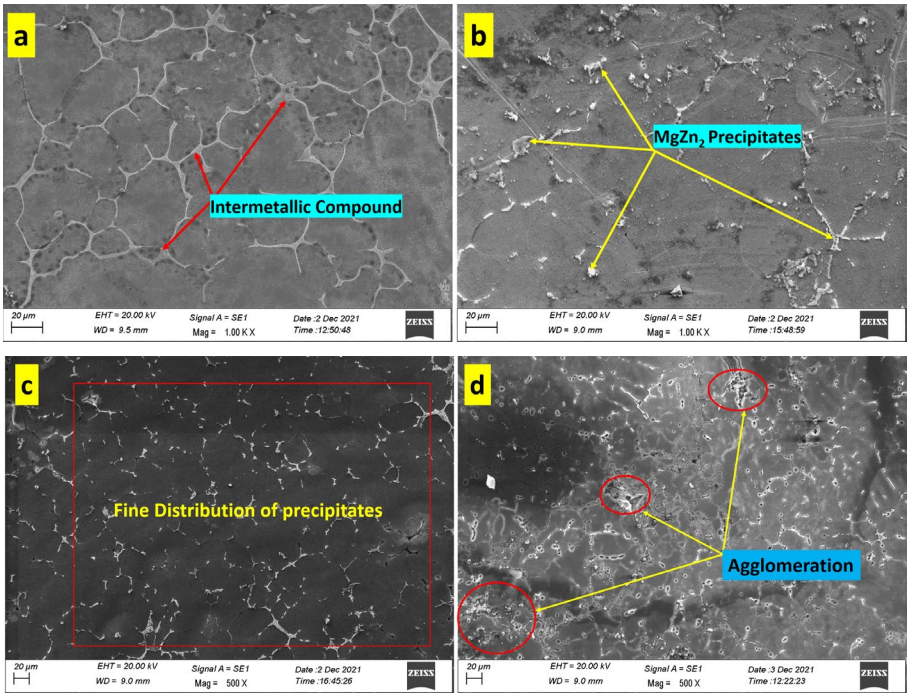

Fig. 4. Microstructure of (a) ACA, (b) HTA, (c) HT-3, (d) HT-4

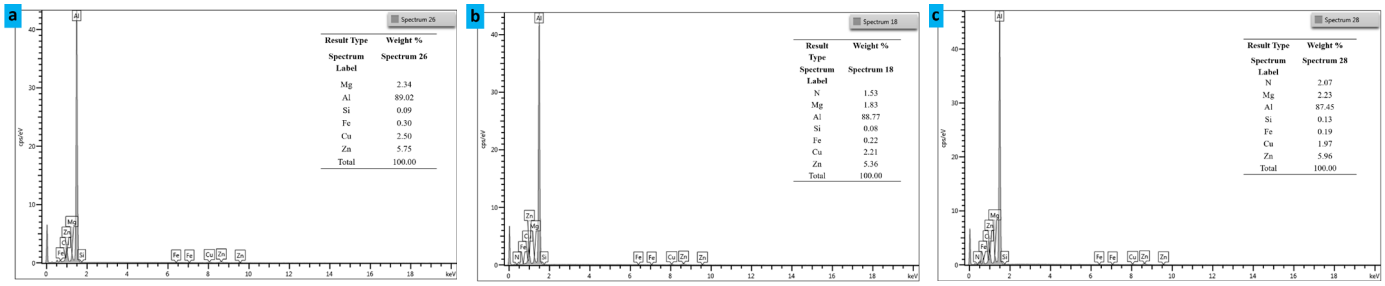

Fig. 5. Energy-Dispersive Spectroscopy plots of (a) ACA, (b) HT-3, () HT-4

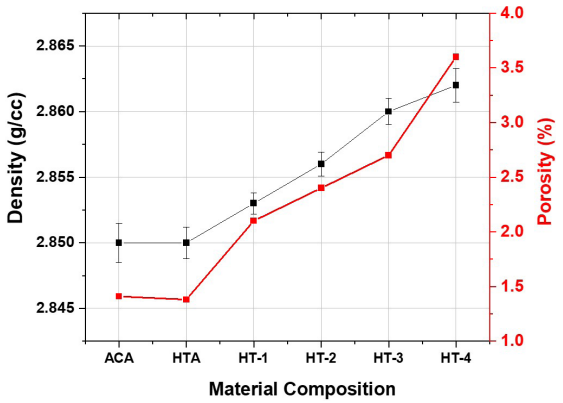

Fig. 6. Density and porosity of as-cast, heat-treated alloy, and nanocomposites

densities of AA7068 and Si_3N_4 are 2.85 and 3.17 g/cc. It is observed that porosity content increases with the addition of reinforcement. SEM confirms the presence of microvoids with the incorporation of nano Si_3N_4 in the Al matrix, resulting in porosity increment. In addition, nanoparticles possess a higher surface area energy because these particles come closer, and their clustering possibility increases, resulting in a micro gap that takes place in between the particles. This phenomenon boosts with increased wt. % of Si_3N_4. Theoretical density is measured from the rule of the mixture and presented in this figure, which shows the increasing trend due to the higher density of reinforcing Si3N4 particles. The current results closely agree with the results reported by [26].

3.3. Optimization of T-6 cycle

A significant difference in hardness was measured in water-quenched and oil-quenched samples (shown in Fig. 7). Water quenched samples are harder than oil quench due to the difference in cooling rate. In comparison, hardness was maximized at 12 h aging for both types. It is observed that the hardness increases with aging time from 2 h to 12 h, then it decreases due to the over-aging

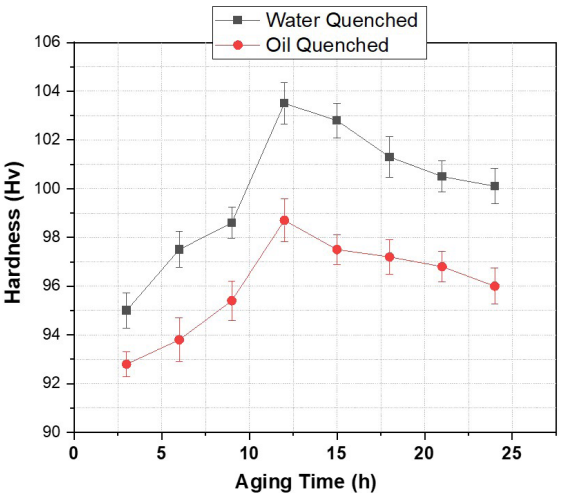

Fig. 7. Hardness of water and oil quenched AA7068

of samples. This hardness behavior related to the formation of $MgZn_2$ precipitates starts during aging; the uniform distribution of fine precipitates is achieved at 12 h aging. After that, the coarsening of $MgZn_2$ precipitates starts, so hardness decreases [27]. Finally, the optimized heat treatment conditions were applied to all compositions, such as solutionizing at 490°C for 6 h, quenching in a water medium, and artificial aging at 140°C for 12 h.

3.4. Hardness

Fig. 8 shows the effect of Si_3N_4 nanoparticles and optimized heat treatment on the hardness of alloy and nanocomposites. It is observed that the hardness increases with the addition of reinforcement from 0.5 to 1.5 wt. %, a decrement in hardness noticed at 2 wt. %. A significant increment in hardness was noticed after performing heat treatment. For AA7068, hardness was observed as 106.5 Hv and 143.8 Hv before and after heat treatment. Significant hardness increment was observed after adding nano Si3N4 particles from 0.5 to 1.5 wt. %. For example, the hardness for HT-3 is 162.3 Hv, i.e., a 12.86% increment compared to HTA. Further addition of Si_3N_4 beyond 1.5 wt. % causes a decrement in hardness value. This increment is attributed to increased dislocation density and load-bearing capacity due to heat treatment and the addition of hard Si_3N_4 nanoparticles, respectively. In addition, the uniform distribution of fine precipitates was achieved after heat treatment, and better particle distribution of nanoparticles observed by stir casting and ultrasonic treatment contributed to hardness increment. Decrement in hardness after 1.5 wt. % due to the increased void content and clustering of particles, as hardness is measured by taking indentation on different locations, so the average value might be affected due to the ununiform distribution of particles.

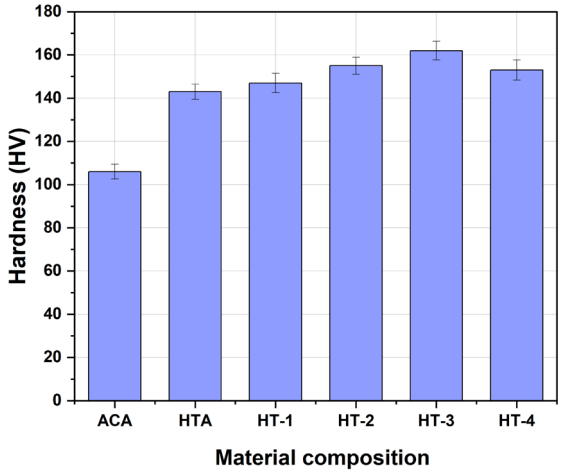

Fig. 8. Hardness of as-cast, heat-treated alloy, and nanocomposites

3.5. Tensile Properties

Tensile properties such as ultimate tensile strength (UTS), yield strength, and percentage elongation of ACA, HTA, and

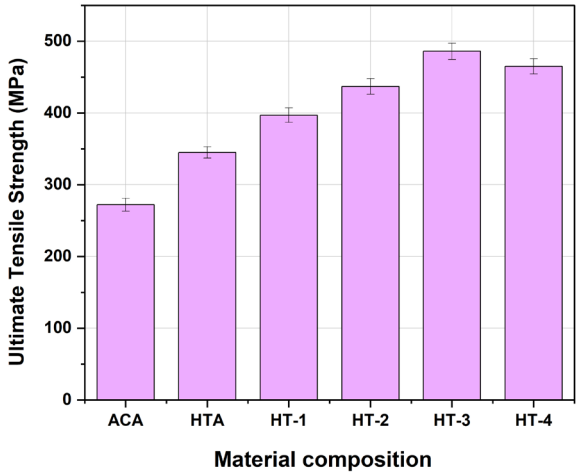

Fig. 9. Ultimate Tensile Strength of as-cast, heat-treated alloy, and nanocomposites

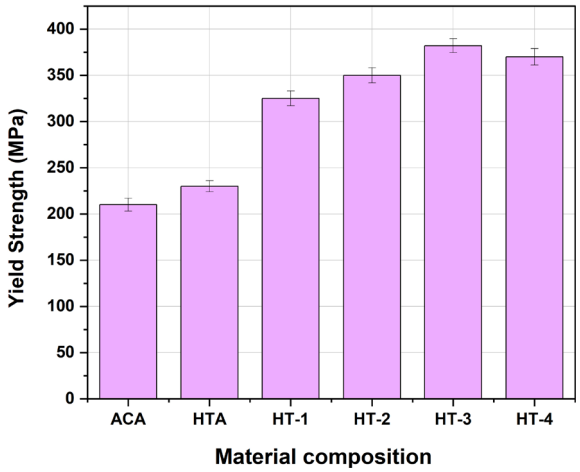

Fig. 10. Yield strength of as-cast, heat-treated alloy, and nanocomposites

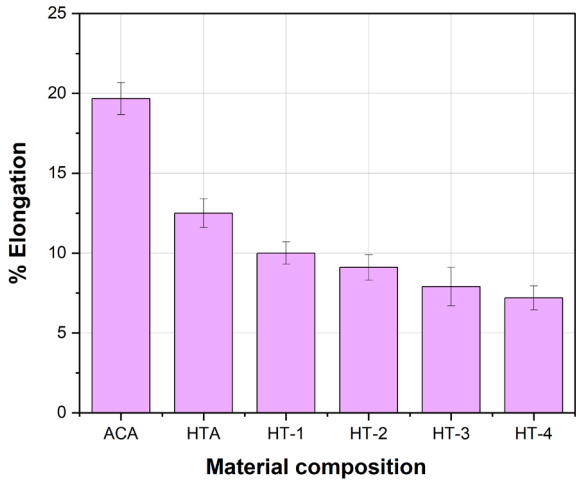

Fig. 11. Percentage Elongation of as-cast, heat-treated alloy, and nanocomposites

nanocomposites are depicted in Figs. 9, 10, and 11. The relation between stress and percentage strain is represented in Fig. 12. It is observed that the UTS and yield strength of ACA significantly enhanced after heat treatment and nano Si_3N_4 addition from HT-1

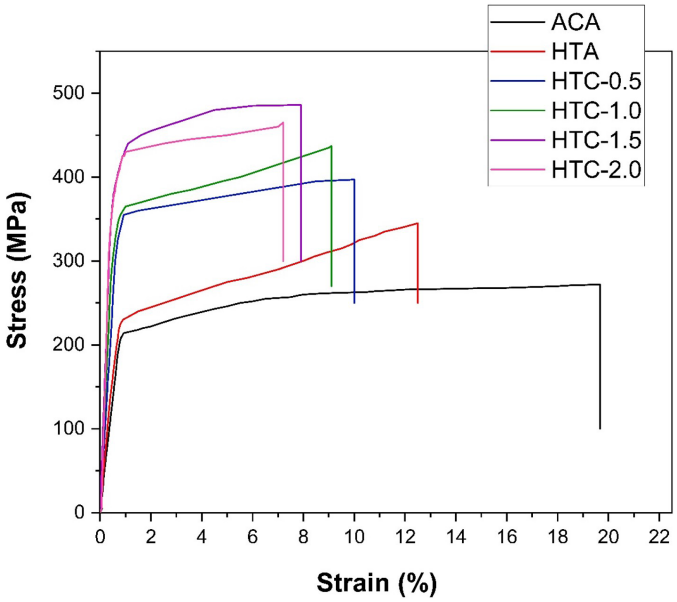

Fig. 12. Stress vs Strain (%) graph

to HT-3. An increment of 40.66 % and 66.08% were noticed in UTS, and yield strength, respectively, for HT-3, compared to HTA. Similarly, the UTS and yield strength of HTA were observed as 345.5 Mpa and 230 MPa, which increased by 27.02% and 9.52%, respectively, after heat treatment compared to ACA.

In contrast, a decrement is noticed in UTS and yield strength for 2 wt. % nanocomposites (HT-4). An increase in tensile strength after reinforcement is attributed to the Hall-Petch, Orowan, thermal mismatch, and load-bearing strengthening. According to hall petch the increase in yield strength of nanocomposites compared to alloy is inversely proportional to grain size; as the grain size reduces, strength increases [28].

It is observed that grain size significantly reduces with reinforcement addition, and minimum size was obtained for HT-4. Still, the increasing trend of tensile strength breaks at HT-4 is due to the increased void content and clustering of nano Si_3N_4. As per orowan the strength increases when nanoparticles are incorporated (as a secondary phase) in monolithic Al alloy. Orowan gives an equation for an increase in strength of nanocomposite compared to alloy, such as $\sigma_y = \sigma_o + Gb/\lambda \ln(D/2b)$ [29], where σ_y and σ_o are yield strength of nanocomposite and alloy, respectively. G, b are alloy's shear modulus and burger vector, respectively. And D, λ are average particle size and interspacing between particles, respectively.

So as the particle size and spacing between nano reinforcement decreases, the strength of the composite would increase. Likewise, the difference in thermal coefficient in Al alloy and Si_3N_4 is responsible for the increment in the dislocation density, and the insertion of nano ceramic Si_3N_4 particles enhances the load-bearing capacity of nanocomposites. Based on the above-mentioned strengthening mechanisms, tensile strength increases with the addition of nano Si_3N_4. An opposite response was noted in composites' ductility; it decreased when Si_3N_4 nanoparticles were added to the alloy and heat treatment. For example, the percentage elongation of ACA is 19.67, which is reduced

by 36.45% for HTA. It is further reduced by adding nanoparticles up to 42.4% for HT-4 compared to HTA. The decrement in ductility is attributed to increased brittleness due to the insertion of ceramic nanoparticles and precipitations [30].

3.6. Fracture surface Analysis

Fracture surfaces of AA7068 alloy in as-cast and heat-treated conditions and heat-treated nanocomposites containing 1.5 and 2.0 wt. % Si_3N_4 (HT-3 and HT-4) were analyzed through FESEM, as shown in Fig. 13. Fig. 13(a) shows the fracture surface of ACA, where grape-like dendrite/dimples and cleavage were observed, indicating the ductile failure of the alloy. In contrast, a lesser number of dimples were noticed in HTA (Fig. 13(b)), with some cleavage panels representing mixed ductile and brittle failure due to the brittle nature of precipitates formed in HTA. Inter-dendrite craking is the prime Mechanism of failure in ACA and HTA during loading. While in the case of HT-3 (Fig. 13(c)), fewer dimples, more facets, and cleavage panels were observed, indicating mixed-mode failure. The load is transferred from the Al matrix to Si_3N_4 reinforcement during tensile loading, resulting in the pulling out of Si_3N_4 particles, which shows good interfacial bonding between particle and matrix. The fracture surface of HT-4 shows in Fig. 13(d), displaying a large number of facets and cleavage panels observed, indicating the brittle fracture due to a large amount of Si_3N_4 nanoparticles. Compared to other nanocomposites, the clustering of Si3N4 particles found in HT-4 is responsible for weaker interfacial bonding resulting in early failure during tensile loading. Breakage of nano reinforcement and interfacial delamination are the prime reasons for failure in the case of nanocomposites. It is concluded that the incorporation of ceramic Si_3N_4 nanoparticles in AA7068 alloy introduces the brittleness and this brittle nature increasing with Si_3N_4 wt. %.

3.7. Summary

Intermetallic compounds such as Al (Zn, Cu, $Mg)_2$ were observed after the solidification of ACA. Whereas, the discontinuous grain boundaries and MgZ_2 precipitates were observed in the microstructure of HTA. In addition, significant refinement of coarser grain was noticed after Si_3N_4 nano reinforcement with uniform distribution of fine MgZ_2 particles in the case of HT-3. Clustering of particles and microvoids was observed in the microstructure of HT-4 due to the higher surface area and low density of Si_3N_4 nanoparticles. The artificial aging duration significantly affected the hardness; peak hardness was obtained after 12 h in both quenching mediums. It was observed that the hardness of water quenched samples is more than oil quench, attributed to a higher rate of cooling due to the higher thermal conductivity of water. The enhancement of mechanical properties with T-6 heat treatment is mainly due to the formation of MgZn2 precipitates and their uniform distribution. In addition, the refinement of grains with nano Si3N4 addition also improves mechanical properties through hall Petch, Orowan, and thermal mismatch strengthening. The fracture surface SEM

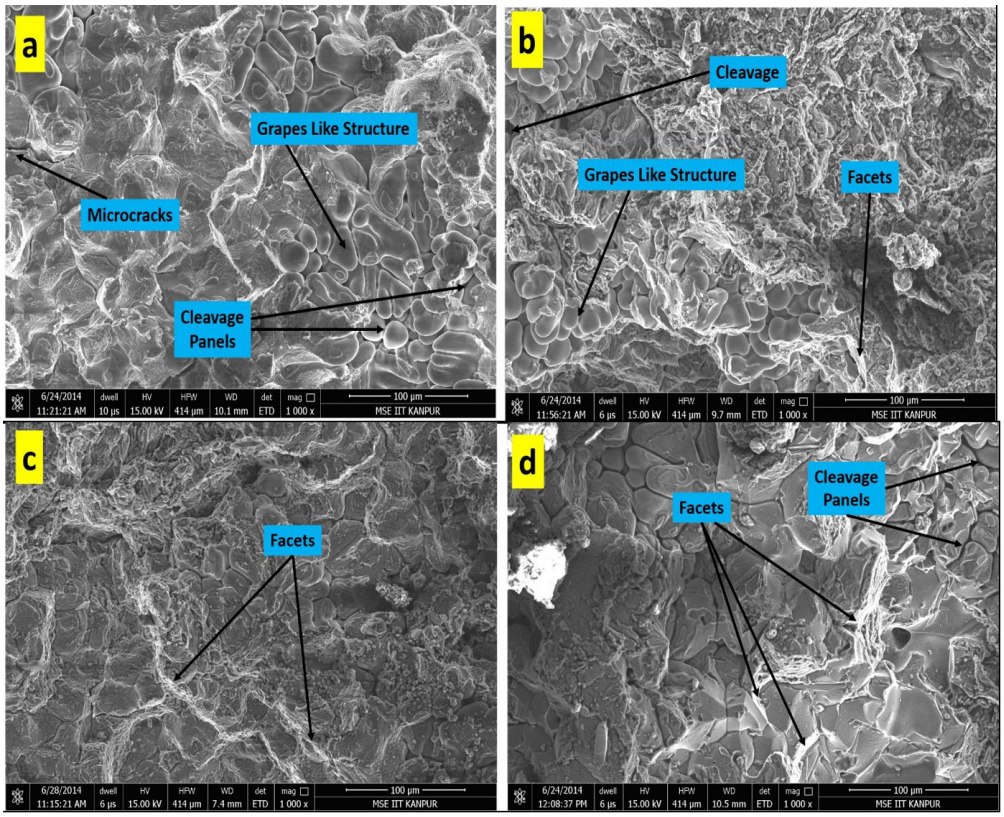

Fig. 13. SEM of Fracture surfaces of (a) ACA, (b) HTA, (c) HT-3, (d) HT-4

revealed as interdendritic cracking is the primary cause of the pure alloy failure, whereas ductile-brittle (mixed mode) failure of nanocomposites assured with the identification of cleavage panels and facets

4. Conclusion

Silicon nitride (Si_3N_4) reinforced AA7068 nanocomposites were successfully developed through stir casting equipped with ultrasonic treatment. The following conclusions were made based on fabrication and characterization:

- T-6 heat treatment cycle was optimized based on hardness analysis for AA7068; maximum hardness was observed for the specimen quenched in water medium and artificial aged at 140°C for 12 h.
- A significant increment in hardness was observed after adding nano Si_3N_4 particles from 0.5 to 1.5 wt. % and heat treatment. For example, the hardness for HT-3 is 162.3 Hv, i.e., a 12.86 and 53.11% increment compared to HTA and ACA, respectively.
- UTS and yield strength of ACA significantly enhanced after heat treatment and nano Si_3N_4 addition from HT-1 to HT-3. An increment of 40.66% and 66.08% were noticed in UTS, and yield strength, respectively, for HT-3, compared to HTA.
- The percentage elongation of ACA is 19.67, which is reduced by 36.45% for HTA. It is further reduced by adding nanoparticles up to 42.4% for HT-4 compared to HTA.
- The fracture of ACA was mainly due to interdendritic cracking (ductile failure), whereas in nanocomposites, ductile-brittle (mixed mode) failure was observed.

REFERENCES

[1] B.R. Sunil, Developing Surface Metal Matrix Composites: A Comparative Survey, Int. J. Adv. Mater. Sci. Eng. **4**, 3, 9-16 (2015). DOI: https://doi.org/10.14810/ijamse.2015.4302

[2] E.A.M. Shalaby, A.Y. Churyumov, A.N. Solonin, A. Lotfy, Preparation and characterization of hybrid A359/(SiC+Si3N4) composites synthesized by stir/squeeze casting techniques, Mater. Sci. Eng. A **674**, 18-24(2016). DOI: https://doi.org/10.1016/j.msea.2016.07.058

[3] R.K. Singh, A. Telang, S. Das, Microstructure , mechanical properties and two-body abrasive wear behaviour of hypereutectic Al − Si − SiC composite, Trans. Nonferrous Met. Soc. China **30**, 1, 65-75 (2020). DOI: https://doi.org/10.1016/S1003-6326(19)65180-0

[4] R.S. Rai, R. Palanivel, J. David Raja Selvam, In-situ synthesis and microstructural characterization of AA6061/(TiB2 + TiC) particles in AA6061 aluminium composite, Mater. Today Proc. **43**, 2255-2258 (2020). DOI: https://doi.org/10.1016/j.matpr.2020.12.533

[5] R.R. Veeravalli, R. Nallu, S. Mohammed Moulana Mohiuddin, Mechanical and tribological properties of AA7075-TiC metal matrix composites under heat treated (T6) and cast conditions, J. Mater. Res. Technol. **5**, 4, 377-383 (2016). DOI: https://doi.org/10.1016/j.jmrt.2016.03.011

[6] H.R. Ezatpour, S.A. Sajjadi, M.H. Sabzevar, Y. Huang, Investigation of microstructure and mechanical properties of Al6061-nanocomposite fabricated by stir casting, Mater. Des. **55**, 921-928 (2014). DOI: https://doi.org/10.1016/j.matdes.2013.10.060

[7] A. Kumar, R.S. Rana, R. Purohit, Synthesis & analysis of mechanical and tribological behaviour of silicon carbide and graphite reinforced aluminium alloy hybrid composites, Mater. Today Proc. **26**, 3152-3156 (2019). DOI: https://doi.org/10.1016/j.matpr.2020.02.650

[8] P. Shao et al., Microstructure and tensile properties of 5083 Al matrix composites reinforced with graphene oxide and graphene nanoplates prepared by pressure infiltration method, Compos. Part A Appl. Sci. Manuf. **109**, 2, 151-162 (2018). DOI: https://doi.org/10.1016/j.compositesa.2018.03.009

[9] A.I. Journal, M. Baghel, C.M. Krishna, Synthesis and characterization of MWCNTs / Al6082 nanocomposites through ultrasonic assisted stir casting technique, Part. Sci. Technol. 1-13 (2022). DOI: https://doi.org/10.1080/02726351.2022.2065651

[10] A. Kumar, R.S. Rana, R. Purohit, Tribological Analysis and Characterization of Zinc Rich Al/Si3N4 Composites Fabricated Via Ultrasonic Assisted Stir Casting Technique, Adv. Mater. Process. Technol. 1-13, (2021). DOI: https://doi.org/10.1080/2374068X.2021.1959111

[11] S.E. Hernández-Martínez, J.J. Cruz-Rivera, C.G. Garay-Reyes, C.G. Elias-Alfaro, R. Martínez-Sánchez, J.L. Hernández-Rivera, Application of ball milling in the synthesis of AA 7075-ZrO2 metal matrix nanocomposite, Powder Technol. **284**, 40-46 (2015). DOI: https://doi.org/10.1016/j.powtec.2015.06.030

[12] M. Irfan, U. Haq, Friction and Wear Behavior of AA 7075-Si 3 N 4 Composites Under Dry Conditions: Effect of Sliding Speed, pp. 0-6, (2018).

[13] S. Kumar Patel, V. Pratap Singh, D. Kumar, B. Saha Roy, B. Kuriachen, Microstructural, mechanical and wear behavior of A7075 surface composite reinforced with WC nanoparticle through friction stir processing, Mater. Sci. Eng. B Solid-State Mater. Adv. Technol. **276**, no. December 2021, 115476 (2022). DOI: https://doi.org/10.1016/j.mseb.2021.115476

[14] R. Clark et al., On the correlation of mechanical and physical properties of 7075-T6 Al alloy, Eng. Fail. Anal. **12**, 4, 520-526 (2005). DOI: https://doi.org/10.1016/j.engfailanal.2004.09.005

[15] J.M. Mistry, P.P. Gohil, Experimental investigations on wear and friction behaviour of Si3N4p reinforced heat-treated aluminium matrix composites produced using electromagnetic stir casting process, Compos. Part B Eng. **161**, no. August 2018, 190-204 (2019). DOI: https://doi.org/10.1016/j.compositesb.2018.10.074

[16] P. Sharma, S. Sharma, D. Khanduja, Production and some properties of Si 3 N 4 reinforced aluminium alloy composites, J. Asian Ceram. Soc. **3**, 3, 352-359 (2015). DOI: https://doi.org/10.1016/j.jascer.2015.07.002

[17] R.K. Singh, A. Telang, S. Das, The influence of abrasive size and applied load on abrasive wear of Al-Si–SiCp composite, Arab. J. Sci. Eng. (2021).
DOI: https://doi.org/10.1007/s13369-021-06349-1

[18] P.J. Mane, K.L.V. Kumar, Study on ageing behaviour of silicon nitride reinforced Al6061 composites, Procedia Eng. **97**, 642-647 (2014). DOI: https://doi.org/10.1016/j.proeng.2014.12.293

[19] C.S. Ramesh, R. Keshavamurthy, B.H. Channabasappa, S. Pramod, Friction and wear behavior of Ni-P coated Si3N4 reinforced Al6061 composites, Tribol. Int. **43**, 3, 623-634, (2010).
DOI: https://doi.org/10.1016/j.triboint.2009.09.011

[20] R. Ambigai, S. Prabhu, Optimization of friction and wear behaviour of Al–Si3N4 nano composite and Al–Gr–Si3N4 hybrid composite under dry sliding conditions, Trans. Nonferrous Met. Soc. China (English Ed.) **27**, 5, 986-997 (2017).
DOI: https://doi.org/10.1016/S1003-6326(17)60116-X

[21] R.K. Singh, A. Telang, S. Das, Abrasive wear response of Al-Si – SiCp composite : Effect of friction heat and friction coefficient, Int. J. Mater. Res. 1-7 (2021).
DOI: https://doi.org/10.1515/ijmr-2020-7869

[22] R.K. Singh, A. Telang, S. Das, Abrasive wear behaviour of as-cast and heat-treated Al – Si – SiCp composite, Int. J. Mater. Res. (formerly Z. Metallkd.) **109**, 1-9 (2018).
DOI: https://doi.org/10.3139/146.111727

[23] J. Li, S. Lü, S. Wu, Q. Gao, Effects of ultrasonic vibration on microstructure and mechanical properties of nano-sized SiC particles reinforced Al-5Cu composites, Ultrason. Sonochem **42**, no. October 2017, 814-822 (2018).
DOI: https://doi.org/10.1016/j.ultsonch.2017.12.038

[24] P.A. Rometsch, Y. Zhang, S. Knight, Heat treatment of 7xxx series aluminium alloys – Some recent developments, Trans. Nonferrous Met. Soc. China **24**, 7, 2003-2017 (2017).
DOI: https://doi.org/10.1016/S1003-6326(14)63306-9

[25] N. Srivastava, G.P. Chaudhari, Microstructural evolution and mechanical behavior of ultrasonically synthesized Al6061-nano alumina composites, Mater. Sci. Eng. A **724**, 199-207 (2018).
DOI: https://doi.org/10.1016/j.msea.2018.03.092

[26] A. Parveen, N.R. Chauhan, M. Suhaib, Study of Si3N4 reinforcement on the morphological and tribo-mechanical behaviour of aluminium matrix composites, Mater. Res. Express **6**, 4 (2019).
DOI: https://doi.org/10.1088/2053-1591/aaf8d8

[27] X.G. Fan, D.M. Jiang, Q.C. Meng, B.Y. Zhang, T. Wang, Evolution of eutectic structures in Al-Zn-Mg-Cu alloys during heat treatment, Trans. Nonferrous Met. Soc. China (English Ed.) **16**, 3, 577-581 (2006). DOI: https://doi.org/10.1016/S1003-6326(06)60101-5

[28] K. Hu, D. Yuan, S. Lin Lu, S. Sen Wu, Effects of nano-SiCp content on microstructure and mechanical properties of SiCp/A356 composites assisted with ultrasonic treatment, Trans. Nonferrous Met. Soc. China (English Ed.) **28**, 11, 2173-2180 (2018).
DOI: https://doi.org/10.1016/S1003-6326(18)64862-9

[29] T.B. Rao, Microstructural, mechanical, and wear properties characterization and strengthening mechanisms of Al7075/SiCnp composites processed through ultrasonic cavitation assisted stir-casting, Mater. Sci. Eng. A **805**, September 2020, 140553 (2021).
DOI: https://doi.org/10.1016/j.msea.2020.140553

[30] N. Srivastava, G.P. Chaudhari, Strengthening in Al alloy nano composites fabricated by ultrasound assisted solidification technique, Mater. Sci. Eng. A **651**, 241-247 (2016).
DOI: https://doi.org/10.1016/j.msea.2015.10.118